

WHAT CAN WE LEARN FROM EXPERIMENTS WITH 10 GEV PHOTONS¹

Jean-Marc Laget

CEA-Saclay, DAPNIA/SPhN, F91191 Gif-Sur-Yvette Cedex, France

ABSTRACT

I review various opportunities to “see” the mechanisms of confinement at work: Meson spectroscopy; Off Forward Parton Distributions in electroproduction of mesons; Gluonic content of hadronic matter in photoproduction of vector mesons; Valence quark wave functions in photoproduction of pseudo-scalar mesons and in Compton Scattering; Short range structure of nuclei in photoproduction of charm near threshold. An intense continuous beam of real photons, in the 10 GeV range, and of electrons, in the 30 GeV range, will allow to address most of these issues.

1. Introduction

One of the fascinating issues in Hadronic Physics is the understanding of the structure of Hadronic Matter at the Confinement Scale. To address it, two ways appear to be very promising. The first is the study of the spectrum and the properties of the mesons. The respective role of the constituent quark-antiquark substructure and of the gluonic content can be disentangled in these simplest systems.

The second way consists to select the simplest quarks and gluons configurations (three valence quarks in baryons, two valence quarks in mesons, three quarks and one or two gluons, etc ...) which are thought to be more amenable to calculations than the full structure of hadrons. This is achieved in *exclusive* reactions involving a large momentum transfer which forces a minimal configuration of partons to be present in the small interaction volume. The study of their subsequent evolution toward a full fledge

¹ Based on invited talks given at the Workshop “Jefferson Lab Physics and Instrumentation with 6-12 GeV Beams” (Newport News, VA, June 15-18, 1998) and the Workshop “Physics With High Energy Real Photons” (Grenoble, France, April 22, 1998).

normal hadron in the nuclear medium provides us with a way to constrain their structure.

In this talk, I will deal with reactions induced by Real Photons (in which case the scale is set by the momentum transfer t , between the incoming photon and the detected meson) as well as with reactions induced by Virtual Photons (in which case the scale is set by the mass squared Q^2 of the virtual photon). After a few remarks on meson spectroscopy, I will start by a survey of our understanding of exclusive reactions induced on nucleon targets, investigate how the study of exclusive reactions induced in the Nuclear Medium may help us to disentangle Hard and Soft mechanisms, and devote the last part of my talk to the study of Charm production near threshold. I will conclude by a discussion of the relevant energy ranges where all these issues may be addressed in the best way.

Needless to say, most of the material in this talk results from an intense activity, over the past few years, to sharpen the physics case and the feasibility of ELFE. I refer the reader to the proceedings of the last Saint-Malo meeting ¹ for a more detailed discussion.

2. Mesons Spectroscopy

A sizable part of this workshop is devoted to define the best ways to investigate the spectroscopy of mesons with an intense beam of real photons. I refer to the corresponding part of the proceedings, and more particularly to Ref. ². Let me comment on a few points more directly connected to the main body of my talk.

The spectrum of the known mesons lie on a few Regge trajectories, of which the slope— about 0.8 GeV^{-2} — appears to be universal and is thought to be related to basic parameters of models of confinement (string tension, strength of the confining potential, etc...). The only notable exception is the Pomeron trajectory, whose the slope is smaller— 0.25 GeV^{-2} . It turns out that a glueball candidate, which have been recently identified ³ in the mass range around 2 GeV , lie on the Pomeron trajectory. This reinforces modelisations of the Pomeron in terms of gluons, which have been proposed ⁴ long time ago and have been revived (see for instance ⁵) by recent findings in diffractive scattering at Hera.

Producing glueballs in electromagnetic interactions may happen to be a challenge. Since electromagnetic probes do not couple directly to glue,

t -channel meson exchange mechanisms are strongly suppressed. u -channel baryon exchange mechanisms in exclusive reactions may prove to be the right way, provided that the nucleon-gluon coupling constant is not vanishing.

3. Exclusive Reactions on a Nucleon Target

Four kinematical regimes are relevant for exclusive reactions induced on nucleon targets:

- Low Q^2 and low t . Below 1 or 2 GeV^2 , the differential cross sections and the various spin observables are well accounted for by the exchange of a few Regge trajectories.
- High Q^2 but low t . Keeping t below GeV^2 , but increasing Q^2 up to 20–30 GeV^2 allows to reach a domain where one can factorize the hard scattering of the photon with the valence constituents of the emitted meson and the non perturbative Off Forward Parton Distributions in the target nucleon ⁶.
- High t but low Q^2 . The other extreme consists to keep Q^2 small (near or at the real photon point) and increase t up to 20–30 GeV^2 . Here, one can factorize the hard scattering of the incoming photon with the valence quarks, of both the target nucleon and the emitted meson, and their non perturbative wave functions.
- High Q^2 and high t . This really perturbative regime may turn out to be almost impossible to reach, due to the smallness of the corresponding exclusive cross-sections.

When going from high to low momentum transfers one really probe the evolution from a description of reaction mechanisms and of the structure of hadrons in terms of valence quarks toward a description in terms of constituent quarks, and hopefully see the confinement mechanisms at work.

Let me illustrate this strategy with a few typical examples.

3.1. Production of Mesons at Large Q^2

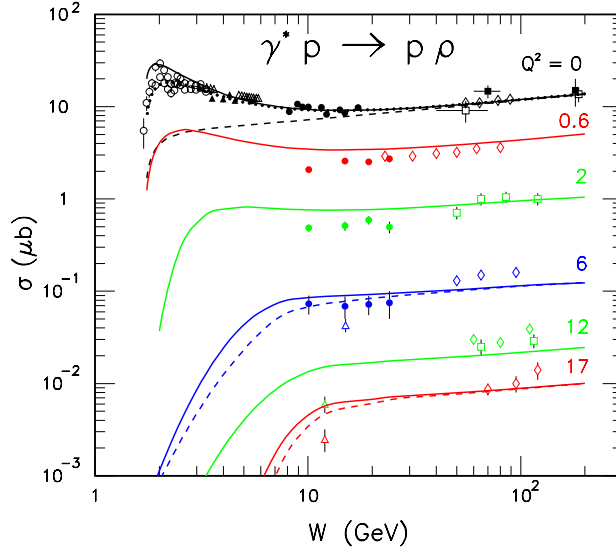


Fig. 1. The cross-section of exclusive electroproduction of ρ meson on nucleon is plotted against the energy in the c.m. system W , for selected values of the four momentum transfer Q^2 .

Fig 1 shows the evolution of the cross-section of the exclusive electroproduction of ρ mesons with the energy available in the c.m. system, and with the mass squared of the virtual photon. The data set spans the range of energies from SLAC and early experiments at DESY (W below 7 GeV) to the present HERA experiments (W up to 200 GeV), covering experiments at CERN and Fermi Lab. (W around $10\text{--}20 \text{ GeV}$). While Pomeron exchange (dashed lines) reproduces fairly well the high energy behavior of the cross-section, f_2 exchange (dotted lines) and to a lesser extent σ exchange (full lines) account for the low energy part.

However this very simple and elegant picture is successful near the real photon point (Q^2 up to $2\text{--}3 \text{ GeV}^2$) but fails to reproduce the increase of the rise of the cross-section with the energy W , observed at high Q^2 . Here, one enters a new domain where the cross sections are rather described by the exchange of two perturbative partons: two gluons at high energy ⁷ or two quarks at low energy ⁸. Fig. 2 illustrates this point when reasonable assumptions are made on the Off Forward Parton Distributions which modelize the probability of finding two partons in the target nucleon.

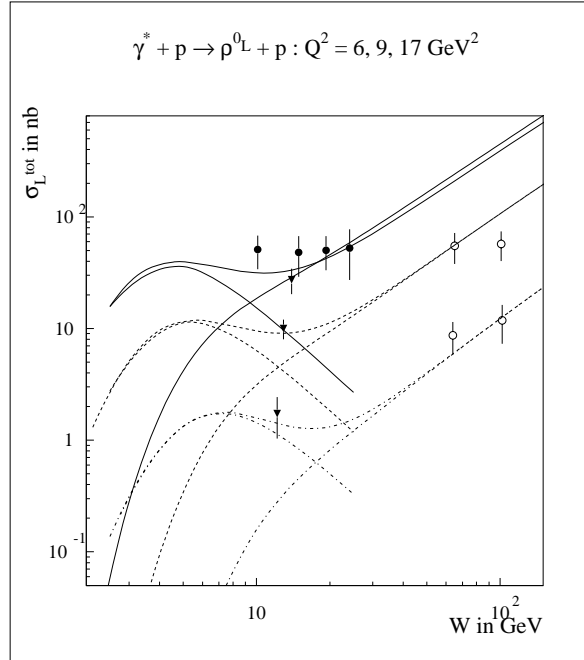


Fig. 2. The cross-section of exclusive electroproduction of ρ meson on nucleon is plotted against the energy in the c.m. system W , at large four momentum transfer Q^2 : 6GeV^2 (full line), 9GeV^2 (dashed line) and 17GeV^2 (dot-dashed line). Quark exchange dominates the low energy sector while gluon exchange dominates the high energy sector.

To day these OFPD's are under lively discussions, as they generalize the parton distributions which are usually extracted from the analysis of inclusive cross-sections in the Deep Inelastic Scattering regime. Their study can be already started at Cebaf, around 6 GeV, will greatly benefit of an energy upgrade to 12 GeV, but will be completed with the advent of a 30 GeV beam. I refer to the talk of M. Guidal⁹ for a more detailed discussion of the corresponding experimental program.

3.2. Production of Mesons at Large t

The other path toward the hard scattering regime lies close or at the real photon point. Here the scale and the hardness of the interaction is set by the momentum transfer t between the incoming photon and the emitted hadrons. This is illustrated in Fig. 3, which shows the angular distribution of the ϕ meson in the exclusive reaction $p(\gamma, \phi)p$.

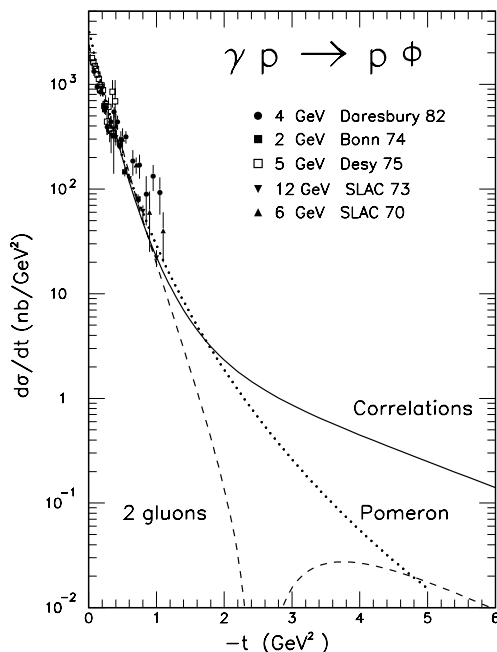


Fig. 3. The cross-section of exclusive photoproduction of ϕ meson on nucleon is plotted against the momentum transfer t , in the energy range 4–10 GeV. Two gluons exchange with and without quark correlations corresponds respectively to the full and dashed lines. The dotted line corresponds to the Pomeron exchange mechanism.

At low momentum transfer t , the exponential slope is fairly well reproduced by the exchange of the Pomeron. At high momentum transfer, one may expect to resolve the structure of the Pomeron into its simplest constituents. Due to the $s\bar{s}$ structure of the ϕ meson, two gluons is the simplest system which can be exchanged in the t channel, provided that no strangeness exists in the nucleon ground state. Two gluon exchange¹⁰ nicely matches Pomeron exchange around $|t| = 1 \text{ GeV}^2$ and exhibits a characteristic node around $|t| = 3 \text{ GeV}^2$. At such a high momentum, the s and \bar{s} quarks are close enough to allow each exchanged gluon to couple either to the same quark or to different quarks inside the ϕ meson. The color singlet nature of the $s\bar{s}$ pair imposes a destructive interference between the two corresponding amplitudes. Note that such a cancellation is at the origin of the mechanism of color transparency (see for instance Ref.¹¹).

Each gluon can also couple to a different quark inside the nucleon, giving access to correlations between quarks in its ground state. I just completed a rough estimate¹² based on a simple model of the quark wave

function in the proton: it turns out to dominate the photoproduction of ϕ at large t . Such a picture seems to be supported by the only data ¹³ available in this range of momentum transfer: Fig. 4 compares the experimental and the theoretical angular distributions of the reaction $p(\gamma, \rho)p$ at 6 GeV.

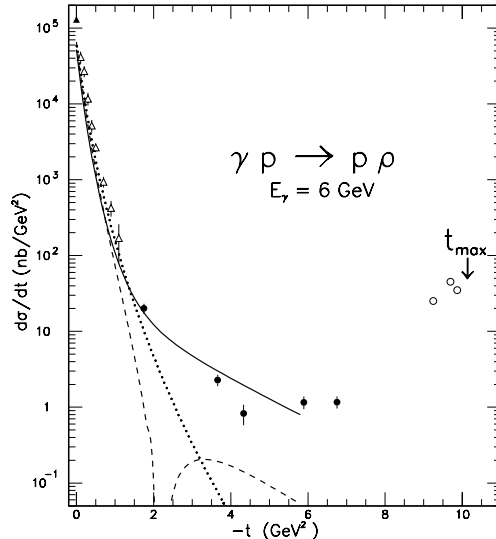


Fig. 4. The same as in Fig. 3, but for ρ production at 6 GeV.

However, besides two gluons exchange, quark interchange mechanisms may contribute to this channel. Also, baryon exchange mechanisms are more important at backward angles in the ρ than in the ϕ production channel (since the ρ -Nucleon coupling constant is much larger than the ϕ -Nucleon one). Finally, the available data set have been obtained with continuous bremsstrahlung beams. For all these reasons a comprehensive experimental study of vector meson production is currently under way at 4 GeV and will be completed at 6 GeV next year at Cebaf ¹⁴. Its extension in the range 10–12 GeV will eventually lead to a better understanding of the Pomeron structure (complementary to diffractive physics at Hera) and provides us with a way to address the issue of quark correlations in the nucleon ground state.

In the pseudo-scalar meson sector, quark interchange mechanisms are thought to be responsible for the reaction cross-sections at large transfer t and u . Here (around 90°) the cross-section of the various photoproduction exclusive channels ¹³ exhibits a scaling behavior (s^{-N}): this is a necessary condition for being in the hard scattering regime. However this not suffi-

cient and no models have been able yet to put such a hard picture on solid grounds. Quark–diquark modelizations of the hadron wave function lead to a fair agreement with the data at the expense of a few reasonable parameters ¹⁵. The only direct calculation ¹⁶ of hard scattering mechanisms suffers from inaccuracy in the treatment of the singularities arising from the on-shell propagation of the partons in the hard scattering amplitude.

To date, Compton Scattering is the only channel where these issues have been addressed in a comprehensive way.

3.3. Compton Scattering

This simplest among the various exclusive channels has received a renewed attention during the past few years. Quark–diquark models ¹⁷ have been worked out in details. An interesting attempt ¹⁸ to model it in terms of OFPD’s has been presented during this meeting. Finally, the hard scattering description ¹⁹ has been improved with a special emphasis on an accurate treatment of the singularities of the matrix element ²⁰.

Fig. 5 compares the predictions of this approach to the sparse available data, for different wave functions of the valence quarks: the asymptotic wave function (bottom solid line) misses the data, while asymmetric wave functions built from sum rules constraints are in better agreement. However, the energy range of the available data may be too low for definite conclusions. The sensitivity to the choice of the wave function is also evident in Fig. 6 which shows the incoming photon asymmetry, for the same choice of the three sum rule wave functions as in Fig. 5.

Provided that the energy is high enough to lie in the hard scattering regime, the question is: To what extent an experimental program can determine the valence quark wave function?

The Compton Scattering amplitude is a convolution of a hard scattering amplitude with the wave functions of the valence quarks in the target and the recoiling proton:

$$\mathcal{M} = \int d[x]d[y]\phi_N^*([y])T_H([x]; [y]; s, t)\phi_N([x]) \quad (1)$$

Expanding the quark wave functions in a polynomial series:

$$\phi_N([x]) = 120x_1x_2x_3(a_{11}+a_{21}x_1+a_{12}x_3+a_{31}x_1^2+a_{13}x_3^2+a_{22}x_1x_2+\dots) \quad (2)$$

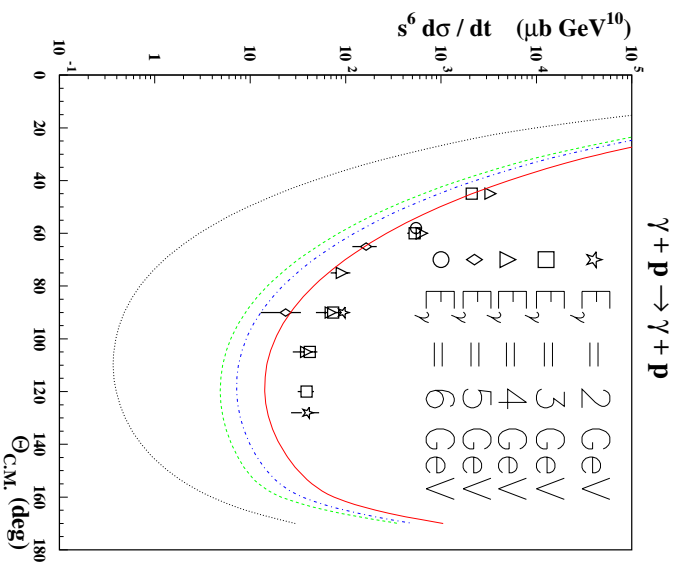


Fig. 5. The differential cross-section of exclusive Compton Scattering.

allows to express the Compton matrix element as a sum of well defined hard matrix elements (the hard scattering amplitude sandwiched between each polynome):

$$\mathcal{M} = \sum a_{ij} a_{kl} T_H(i, j, k, l) \quad (3)$$

of which the coefficients are to be determined by the experiment.

Starting from one of the sum rule wave functions ²¹, pseudo-data have been generated from the theoretical prediction of Eq. 1, and analyzed in order to extract the various coefficients a_{ij} and compare them to their input values, for different assumptions on the accuracy of the measurement.

A typical result is shown in Fig. 7. It clearly shows that not only an accuracy of $\pm 1\%$ must be achieved, but that the simultaneous inclusion of polarized observables in the analysis is mandatory! I refer to Ref. ²⁰ for a more detailed account of works along these lines.

Such a goal is not out of reach, thanks to the progresses which have been made, or are expected, in the production of polarized tagged photon beams. A preliminary estimate ²² shows that the goal of an accuracy of 2%,

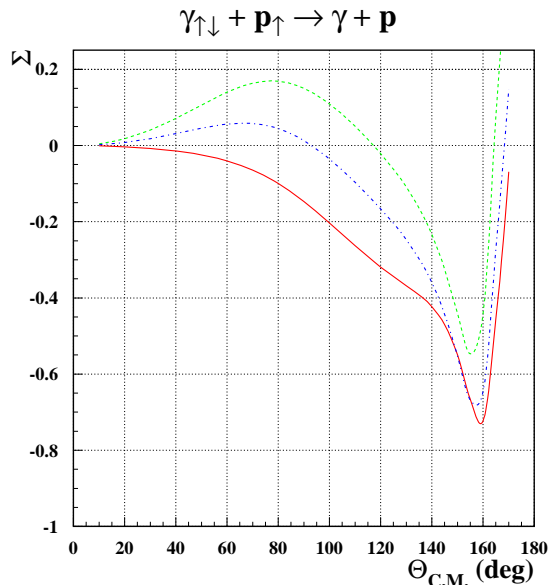


Fig. 6. The incoming photon asymmetry in exclusive Compton Scattering.

on the differential cross-section and asymmetries at 90° , can be reached in 120 days with a photon flux of $N_\gamma = 10^8 \gamma/s$ on a $2g/cm^2$ target, at 12 GeV ($s = 23GeV^2$). This sets the highest useful energy of a real photon beam: above, the cross-sections are too low to allow meaningful studies of exclusive reactions.

The issues related to the design of such a photon beam are currently addressed within the Real Photon Working Group of the European Network HaPHEEP (Hadronic Physics with High Energy Electromagnetic Probes): a pre-conceptual design report is foreseen by the spring 1999.

4. Exclusive Reactions in Nuclei

The key question is therefore: At which momentum transfer hard scatterings dominate the reaction amplitude? This is still an open issue which is under fierce debates. Color Transparency may prove to be the most direct way to answer it.

At other extreme, one may ask how to address issues related to the short range structure of nuclear matter by mean of hard scattering mechanisms.

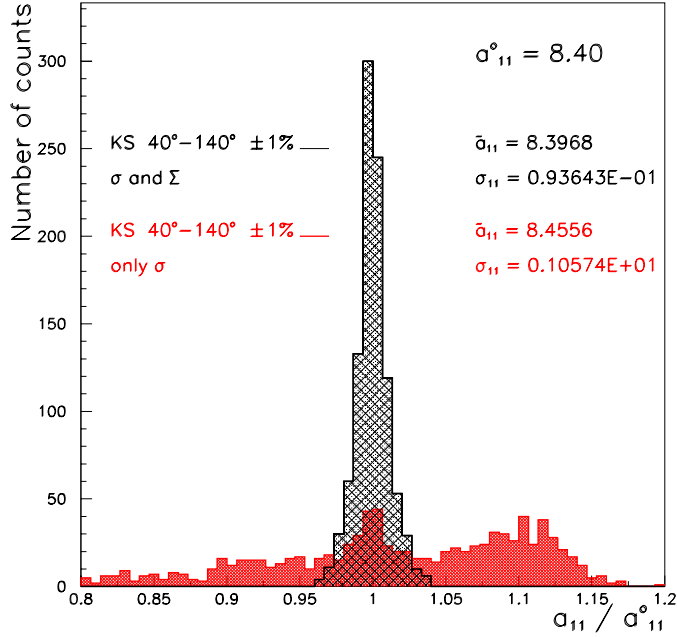


Fig. 7. The determination of the coefficient a_{11} when only the unpolarized cross-section is used (flat area) and when both unpolarized and unpolarized cross-section are used (peak).

4.1. Color Transparency

The concept of “Color Transparency” follows from the underlying structure of QCD: interactions between “white” objects depend on their transverse size. A hard scattering of the probe produces recoiling particles with small transverse size, whose the subsequent interactions in Nuclear Matter are reduced. There is no doubt that Color Transparency should occur. The question is where and when.

The idea is to select one of the simplest configurations of a nucleon (or a hadron) in a nucleus and to see how it evolves toward its asymptotic wave function. The study of the interaction of the outgoing hadron with the nuclear medium, as a function of the size of the nucleus, will give us informations on the corresponding evolution. However, the characteristic scale of the evolution should be larger, or comparable, to the size of the

largest nuclei.

To date there are no convincing evidences for Color Transparency. The reason is that most of the attempts were performed in quasi elastic kinematics. In the $A(e,e'p)$ reactions, for instance, it is very likely that the values of Q^2 are too low to observe color transparency in the quasi-free kinematics channels, where the energy of the ejected nucleon T_p and the photon four-momentum are not independent ($T_p = Q^2/2M$). In the range of reasonable values of Q^2 , for which the cross section does not vanish, the life time of the small object is of the order of the distance between nucleons rather than the nuclear radius. For instance, at the highest $Q^2 = 6 \text{ GeV}^2$ where data exist, the energy of the outgoing proton is only 3 GeV and its characteristic evolution distance is no more than 1.5 fm.

4.2. Color Transparency in Few Body Systems

The way to overcome this difficulty is to study reactions induced by photons or electrons in few body systems: Exclusive reactions allow to adjust the formation length of the hadron to the distance between nucleons. The kinematics should be chosen such that the interactions of the emerging hadron with a second nucleon are maximal. This occurs when the produced hadron propagates on-shell (triangular logarithmic singularity). A clear signal for color transparency would be the suppression of final state interactions when the momentum transfer increases.

As an example, Fig. 8 shows such a signal in the case of the $D(e, e'p)n$ reaction. When the recoiling neutron momentum is high enough (about 400 MeV/c or higher), the quasi free process is suppressed and Nucleon-Nucleon rescattering dominates the cross-section: it is maximum when $X = Q^2/2m\nu = 1$. This is a clear signal which depends only upon on shell matrix elements and upon the low momentum components of the nuclear wave function: The starting point is founded on solid grounds. When Q^2 increases, one select configurations in the nucleon with smaller and smaller transverse extension, which interact less likely with the second nucleon: it is expected that the on-shell rescattering peak disappears above a certain momentum transfer.

This situation is more comfortable than in the more classical study of quasi elastic scattering of electrons from heavy nuclei, where one look for a change of a flat level of attenuation of the outgoing nucleon, instead of the

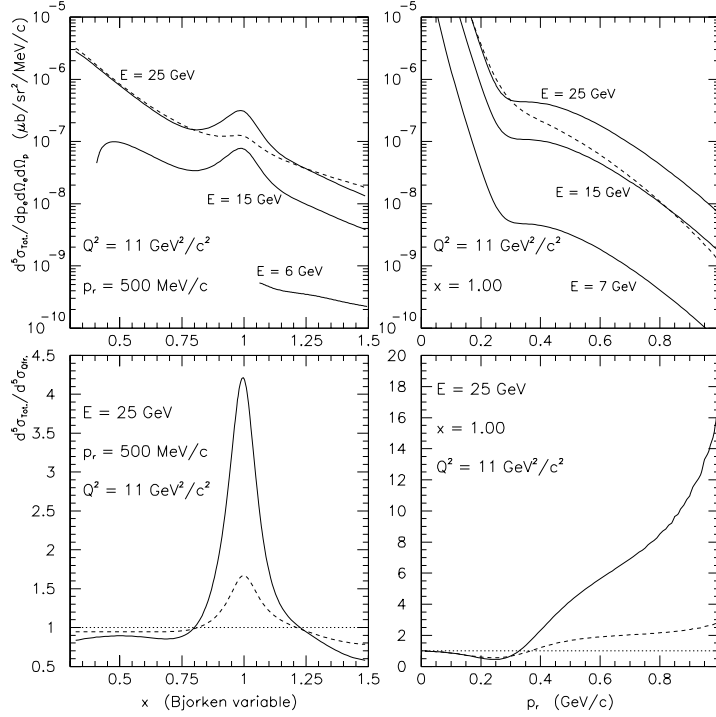


Fig. 8. Fully differential cross-section (top) and ratio of the total to the quasi-free cross section (bottom) of the $D(e, e'p)n$ reaction. The left panels correspond to constant neutron recoil momentum P_r . The right panels correspond to constant $X = q^2/2M\nu$. The full lines and dashed lines include nucleon rescattering without and with color transparency effect, respectively. The dotted curves correspond to the quasi-free process.

evolution of a well defined peak.

Counting rate estimates²³ have been performed in the context of the ELFE project. They show that, for an energy around 30 GeV, the signal can be extracted up to $Q^2 \simeq 20 \text{ GeV}^2$, provided a luminosity of $\mathcal{L} = 10^{38} \text{ cm}^{-2} \text{ s}^{-1}$ is achieved when two well shielded magnetic spectrometers are used, or $\mathcal{L} = 10^{35} \text{ cm}^{-2} \text{ s}^{-1}$ in the case of a 4π detector. An experiment has been approved at CEBAF²⁴, but only $Q^2 = 6 \text{ GeV}^2$ will be reached there

The onset of Color Transparency will indicate the range of momentum transfer where hard scatterings dominate the reaction amplitude: it may well depend on each channel.

4.3. Production of Pseudoscalar Mesons

It may occur earlier in Photo and Electroproduction of Mesons. The reason is that these channels lie in between Deep Inelastic Scattering (DIS) and Elastic Scattering (Form Factors). In DIS the energy transfer is large enough to break-up the target, making a hard scattering description good enough at momentum transfers as low as $Q^2 \simeq 1 \text{ GeV}^2$. On the contrary, the energy transfer is vanishing in form factor measurements, rendering questionable a hard scattering description at low momentum transfers, in the range of few GeV^2 . In exclusive mesons production reactions, both the energy and the momentum transfers are large enough to allow for a perturbative treatment in the momentum transfer range of few GeV^2 .

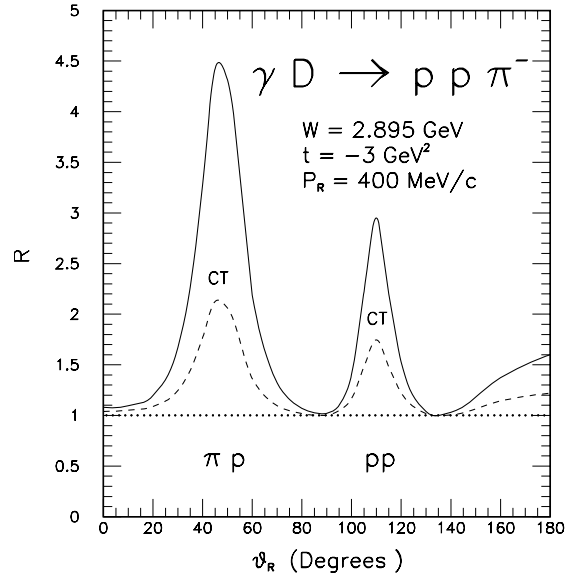


Fig. 9. Ratio of the total to the quasi-free cross section of the $D(\gamma, \pi^- p)p$ reaction against the angle of the recoiling proton whose the momentum is kept constant at 400 MeV/c. The peak at the left corresponds to πp rescattering, while the peak at the right corresponds to pp rescattering. The full lines and dashed lines include hadron rescattering without and with color transparency effect, respectively. The dotted curves correspond to the quasi-free process.

A good example is the reaction $D(\gamma, p\pi^-)p$ in the energy range $4 < E_\gamma < 10 \text{ GeV}$. For real photon the momentum transfer t , between the incoming photon and the outgoing pion, sets the size of the interaction volume. As can be seen in Fig. 9, the on shell rescattering peaks corresponding

to πp or pp interactions are clearly separated. At the top of each peak, the rescattering amplitude is dominated by low momentum components of the deuteron wave function and on mass shell elementary reaction amplitudes (see Ref. ²⁵): Such a Logarithmic singularity has already been observed at lower energies ²⁶. Furthermore, the elementary reaction $n(\gamma, \pi^-)p$ is almost flat, in the range of t around 3 to 10 GeV^2 , and exhibits, around $\theta_\pi = 90^\circ$, a scaling behavior which is a necessary condition for hard scatterings. Here, the nucleon cross section is well reproduced by a model based on the exchange of saturating Regge trajectories ²⁷.

Figs. 10 and 11 show the evolution of the cross-sections at the top of the πp rescattering peak against the recoil momentum P_R and the momentum transfer t , respectively. The expected effect of Color Transparency is clearly apparent. A toy model, based on a geometrical expansion of the mini configuration of the ejected hadron, has been used and is meant as a guide: Only experiment will tell us what is the relevant nature of the process which governs its evolution and formation.

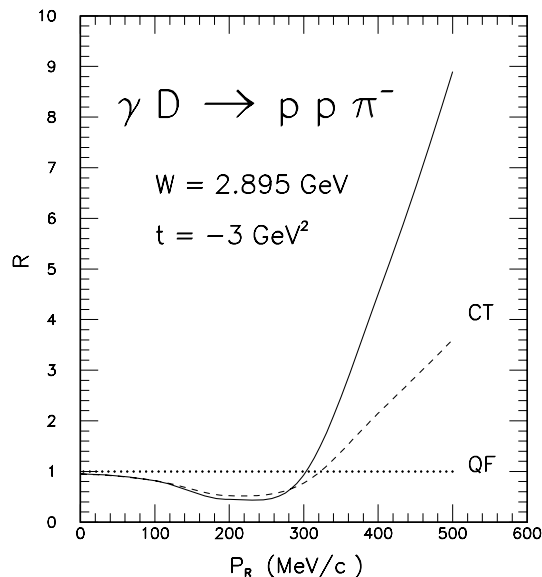


Fig. 10. Ratio of the total to the quasi-free cross section of the $D(\gamma, \pi^- p)p$ reaction against the momentum of the recoiling proton, at the top of the πp rescattering peak. The full lines and dashed lines include πp scattering without and with color transparency effect, respectively. The dotted curves correspond to the quasi-free process.

Counting rate estimates show that this channel is already accessible in

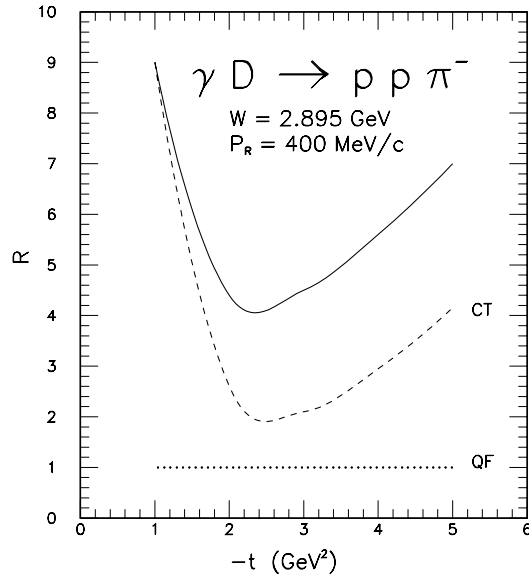


Fig. 11. Same as in Fig. 10, but against the momentum transfer.

the CLAS detector at CEBAF, in the range of t around 3 to 5 GeV^2 . A beam of real photons of 10 GeV would be ideal to map out the t dependence up to 10 GeV^2 . Above, the cross sections are decreasing too fast (as s^{-7}), making the measurement almost impossible.

4.4. Production of Vector Mesons

Exclusive Vector Mesons production on few body systems is certainly very promising. It allows to prepare a pair of quarks, with an adjustable transverse size, and to study its interaction with a nucleon in well defined kinematics. Furthermore, the coherence time (during which the incoming photon oscillates into a $q\bar{q}$ pair) and the formation time (after which this pair recombines into the final meson) can be adjusted independently to the internucleon distance. Such a study may end up with a better understanding of the formation of vector mesons in cold hadronic matter, and is complementary to the study of vector meson production in heavy ion collisions. Although more work has to be done to put it on the same footing as the previously discussed channels, the strategy will follow the same lines: the elementary cross sections are of same order of magnitude.

A special emphasis should be put on ϕ and J/Ψ mesons production: not only these narrow states are more easy to identify, but their flavor content, different from that of the ground state of cold hadronic matter, makes them a promising probe.

4.5. Short Range Properties of Nuclei

Instead of using the well established long range properties of a nucleus as a filter to pin down hard scattering mechanisms, one may alternatively take advantage of the short range nature of hard processes to unravel some aspects of the short distance behavior of nuclei. Among many possibilities, let me emphasize three axis of research.

One of the fascinating issues in Nuclear Physics is that the conventional constituents of nuclei appear to keep their identity, even if the nucleus is shaken by a photon of very high energy. The best example is the two body photodisintegration of the deuterium, of which the scaling of the cross-section with the energy, previously observed at SLAC ²⁸ up to 2 GeV, has recently been confirmed at energies above 3 GeV at Cebaf ²⁹. Of course, this occurs in a tiny part of the available phase space, but corresponds to the excitation of a highly excited intermediate state which couples to the short range part of the initial deuteron and the final two nucleon system. Understanding such a mechanism requires a comprehensive study not only of the unpolarized cross-section of the photodisintegration of the few body systems, but also of the various spin observables.

The second issue concerns exotic configurations which may occur at short range in the few body systems. In deuterium, for instance, instead of projecting onto two white clusters (the nucleons) the six quarks may also project onto two colored clusters which eventually couple to a white deuterium. Such a hidden color configuration may be revealed in ϕ photoproduction off deuterium: each of the two exchanged gluons can couple to a different colored cluster, transforming it in a white nucleon which is detected in the final state. The physics case is developed in Ref. ¹⁰ which I refer the reader to.

Last, the response of nuclei at $X > 1$ is still an open issue. Here, for kinematical reasons, only nucleons can be ejected, but free nucleon kinematics are forbidden: this opens a window on short range mechanisms. A comprehensive study requires not only electron beams of high intensity, since

the corresponding cross-sections are very small, in the 12 GeV range ³⁰ but will benefit greatly of the study of selected spin observables.

5. Production of Charm Near Threshold

It is the large mass of the charmed quark which sets the scale of the interaction: contrary to the light quark sectors, hard scattering mechanisms are already at work at the real photon point, even at low momentum transfer t .

Fig. 12 illustrates this point. While the exchange of a few Regge trajectory leads to a fair agreement with the data in the light quark sector over a wide range of energies, this fails completely to account for the J/Ψ production. As in the case of ρ production at large Q^2 (Fig. 1), the Pomeron exchange contribution exhibits a flat behavior, and the step rise of the data with W can only be accounted for by the exchange of two perturbative gluons ³¹. In both cases similar hard scatterings are at work.

Near the J/Ψ threshold, the production mechanism may be less simple (a 10–12 GeV photon beam is just above). Since both the two charmed quarks and the three valence quarks happen to be in the same small interaction volume, three gluon exchange may be as important as two gluon exchange. However, the formation time of the J/Ψ meson is long enough to allow the study of the interaction and the evolution of a $c\bar{c}$ pair in cold hadronic matter. This may have implications ranging from the search of Quark-Gluon Plasma to the existence of possible charmed bound states.

But one the most appealing window is the possibility to reveal and study “hot spots” or compact subnuclear objects in charm production below threshold in nuclei. The elementary interaction is hard enough to select possible compact multiquark states in a kinematical regime inaccessible on free nucleon targets.

All these idea have been beautifully presented elsewhere ³², which I refer the reader to. Designing an experimental program is a task which remains to be performed in the next few years.

6. Conclusion

To conclude, exclusive reactions induced on nucleon targets will offer

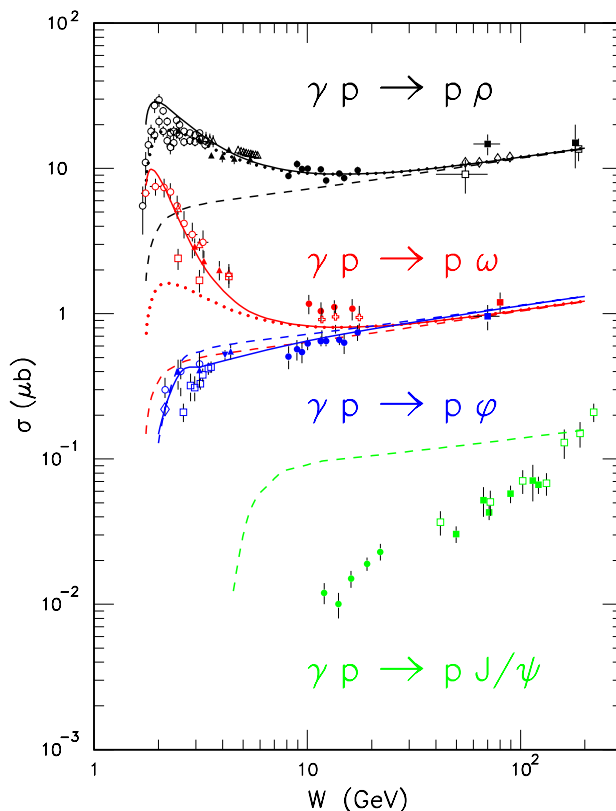


Fig. 12. The cross-section of the photoproduction of the various vector mesons is plotted against the c.m. energy W . Dashed lines include the Pomeron exchange only. Dotted curves include also f_2 exchange. The full curves include also σ exchange (ρ production) or π exchange (ω production).

us with an unique window to track (to “see”) confinement mechanisms at work: production of exotic mesons (glueballs, etc. . .) and exchange of, free or bound, partonic systems.

Exclusive reactions induced in the few body systems may well be the best place to study the onset of color transparency and its relationship to hard scattering mechanisms. The key issue is to select kinematics where rescatterings between hadrons are maximized and are described without any uncertainty: this provides a safe starting point for determining the evolution of scattering cross sections with the momentum transfer.

An intense continuous beam of real photons of about 10 GeV will be ideally suited: above the exclusive reaction cross-sections decrease too quickly to be measured. However, a continuous beam of electrons of 30 GeV is

necessary to map out the Q^2 dependency of the various channels.

The corresponding experimental program can be started at CEBAF, in its present 6 GeV configuration, and fully justifies an upgrade up to 12 GeV.

The step toward 30 GeV requires a coherent effort of the community. To day, two paths are open: either continue the energy increase on the Cebaf site, or take advantage of the opportunity to built ELFE@DESY ¹. It is very likely that the final choice will result from a world-wide decision making process.

7. Acknowledgements

This work was supported by the French Atomic Energy Commission (CEA) and in part by the European Commission (EC) under contract ERB FMRX-CT96-0008.

8. References

1. N. d'Hose et al., Eds. "Prospects of Hadrons and Quark Physics with Electromagnetic Probes". Saint-Malo, France, Sept. 23-27, 1996. Nucl. Phys. A622 (1997) Nos 1,2.
2. A. Dzierba, these proceedings.
3. S. Abatzis et al., Phys. Lett. B324 (1994) 509.
4. S. Nussinov, Phys. Rev. Lett. 34 (1975) 1286; F.E. Low, Phys. Rev. D12 (1975) 163
5. A. Donnachie and P. Landshoff, E-print hep-ph/9806344, June 1998.
6. J. C. Collins, L. Frankfurt and M. Strikman, Phys. Rev. D56 (1997) 2982.
7. L. Frankfurt, W. Koepf and M. Strikman, Phys. Rev. D54 (1996) 3194; S. J. Brodsky et al., Phys. Rev. D50 (1994) 3134.
8. M. Vanderhaeghen, P.A.M. Guichon and M. Guidal, Phys. Rev. Lett. 80 (1998) 5064.
9. M. Guidal, These Proceedings.
10. J.-M. Laget and R. Mendez-Galain, Nucl. Phys. A581 (1995) 397.
11. J.F. Gunion and D. Soper, Phys. Rev. D15 (1977) 2617.

12. J.-M. Laget, in preparation.
13. R.L. Anderson et al., Phys. Rev. D4 (1971) 1937.
14. G. Audit et al., Cebaf Experiment 93-031.
15. P. Kroll et al., Phys. Rev. D55 (1997) 4315.
16. G. Farrar et al., Nucl. Phys. B349 (1991) 655.
17. P. Kroll et al., Nucl. Phys. A598 (1996) 435.
18. A. Radyushkin, These Proceedings.
19. G. Farrar and H. Zhang, Phys. Rev. D41 (1990) 3348; Phys. Rev. D42 (1990) 2413E.
20. M. Vanderhaeghen, P. Guichon and J. Van de Wiele, Nucl. Phys. A622 (1997) 144c.
21. I.D. King and C.T. Sachrajda, Nucl. Phys. B279 (1987) 785.
22. N. D'Hose, private communication.
23. E. Voutier et al., contribution to the parallel sessions of the Saint-Malo ELFE Workshop, Saclay Report DAPNIA-SPhN-96-35, 1996.
24. K.S. Egiyan et al., Cebaf Experiment 94-019.
25. J.-M. Laget, Phys. Rep. 69 (1981) 1.
26. P.E. Argan et al., Phys. Rev. Lett. 41 (1978) 86.
27. M. Guidal, J.-M. Laget and M. Vanderhaeghen, Phys. Lett. B400 (1997) 6; Nucl. Phys. A627 (1997) 645; Phys. Rev. C57 (1998) 1454.
28. J. Napolitano et al., Phys. Rev. Lett. 61 (1988) 2530.
29. R. Holt et al., Cebaf Experiment 89-012.
30. O. Bing et al., Conference Proceeding 44 "The ELFE Project"; J. Arvieux and E. De Sanctis Eds., SIF, Bologna 1993, p. 475.
31. M.G. Ryskin et al., Z. Phys. C76 (1997)231.
32. P. Hoyer, Nucl. Phys. A622 (1997) 284c.